JMEPEG (2012) 21:345–352
DOI: 10.1007/s11665-011-9903-6

1059-9495/$19.00

Effects of Nb on the Microstructure and Mechanical Properties of Water-Quenched F_{GBA}/B_G Steels

Guhui Gao, Chun Feng, and Bingzhe Bai

(Submitted September 7, 2010; in revised form January 19, 2011)

In order to reduce the alloying cost, Mn-series low carbon water-quenched grain boundary allotriomorphic ferrite (F_{GBA})/granular bainite (B_G) steels have been developed. The effect of 0.06 wt.% Nb on microstructure and mechanical properties of F_{GBA}/B_G steel was investigated. The result showed that the addition of 0.06 wt.% Nb improved the hardenability of the F_{GBA}/B_G steel, refined the grain size of F_{GBA}, promoted the granular bainitic transformation, and refined the granular bainite including its bainitic ferrite and martensite/austenite (M/A) constituents. With the addition of 0.06 wt.% Nb, the yield strength increased from 560 to 741 MPa, and the impact energy increased from 93 to 151 J, respectively, for 30-mm thickness steel plates. It is supposed that the addition of 0.06 wt.% Nb could improve the mechanical properties of the F_{GBA}/B_G steel by refining the microstructure and increasing the amount of strengthening phases.

Keywords granular bainite, low carbon steel, mechanical properties, Nb alloying, phase transformation

1. Introduction

To obtain excellent combination of strength, toughness and weldability, the high strength low alloy (HSLA) steel plates have been developed to replace conventional medium carbon steels in the last two decades (Ref 1-7). Alloy additions such as Mo, Ni, Cr, and Cu are commonly added in HSLA steels in order to increase the hardenability of austenite. However, high alloying cost limits the application of these steels. In order to eliminate very expensive elements such as Ni, Mo, and Cr from the chemical composition of the steels, Mn-series low carbon bainitic steels have been developed (Ref 8). In particular, dual-phase microstructure with F_{GBA} and B_G shows good combination of strength, toughness, and weldability (Ref 9-11). F_{GBA}/B_G steel has been designed according to the duplex microstructure strengthening and toughening theory. Since the strength of granular bainite (B_G) structure is much higher than that of pearlite structure, substituting pearlite with B_G in ferrite-pearlite (F/P) steel will evidently increase steel strength. On the other hand, the proeutectoid ferrite in F_{GBA}/B_G steel is able to obtain the better plasticity and toughness with grain boundary allotriomorphic ferrite (F_{GBA}) except the network-like ferrite and widmannstatten ferrite. Hence, the small grain-size discontinuous grain boundary allotriomorphic ferrite (F_{GBA}) as one constituent phase is used to improve the toughness of F_{GBA}/B_G steel (Ref 12). However, the main alloying elements, such as C, Mn, or Cr must be added in order to increase the strength of air cooled F_{GBA}/B_G steel, which is harmful to the weldability and toughness.

Accelerated cooling in thermo-mechanical controlled process (TMCP) is now widely recognized as a means to obtain high strength in association with superior toughness and formability (Ref 5, 7, 13). This behavior is associated with the influence of cooling rate on the transformation of austenite into different microstructural constituents, which ultimately determine the final properties. In this regard, accelerated cooling enables strengthening of the steels with low carbon content and simultaneously obtain superior toughness. Therefore, water-quenched Mn-series bainitic steels were put forward, and the dual phase microstructure with F_{GBA} and B_G can be obtained during cooling rate of 30 to 0.33 °C/s for Mn-series low carbon bainitic steels without Cr addition. In other words, it is suggested that low carbon F_{GBA}/B_G steel plates with thickness of 20-120 mm can be turned out through water quenching.

It is well known that the addition of niobium in steels has profound effects on strengthening through grain refinement and precipitation hardening without sacrificing weldability in HSLA steels (Ref 14-16). Unfortunately, no quantitative data are yet available on the way that Nb affects the microstructure and mechanical properties of water-quenched low carbon F_{GBA}/B_G steels.

The present investigation is mainly focused on the effect of 0.06% Nb alloying on the microstructure and mechanical properties of water-quenched F_{GBA}/B_G steel plates with 30 mm thickness. The objective was to study the reason why the addition of Nb improves mechanical properties from determining CCT curves and characterizing microstructure evolutions of water-quenched F_{GBA}/B_G steel.

2. Materials and Experimental Procedure

The chemical compositions of the experimental steels are listed in Table 1. The steels were melted in a vacuum induction

Guhui Gao and **Bingzhe Bai**, Department of Materials Science and Engineering, Tsinghua University, Beijing 100084, China; and **Chun Feng**, Tubular Goods Research Center of CNPC, Xi'an 710065, China. Contact e-mail: gaogh08@mails.tsinghua.edu.cn.

furnace. The ingot was forged into square bars with dimension of 60 × 60 × 130 mm. The bars were reheated at 1250 °C for 1 h. The deformation process was 60 mm $\xrightarrow{20\%}$ 48 mm $\xrightarrow{21\%}$ 38 mm $\xrightarrow{21\%}$ 30 mm and the finish rolled temperature was 800 °C. After hot rolling, the steel plates were immediately water quenched to 450 °C, and then air cooled to room temperature.

Cylindrical samples of 15 mm in height and 10 mm in diameter machined from the rolled plates were used for thermomechanical simulation carried out on Gleeble-1500 thermomechanical simulator. The CCT curves were determined through the following procedure that the cylindrical samples were reheated at 1250 °C for 5 min, cooled to 850 °C at 1 °C/s, deformed with reduction of 30%, and then cooled to room temperature at different cooling rates. According to the results of dilatometric measurements and the microstructure observations, the CCT curves of the steels can be plotted.

Tensile and Charpy impact specimens were obtained from the 1/2 thickness location of rolled plate. Round tensile specimens with a gage diameter of 5 mm and a gage length of 30 mm were prepared in the transverse direction, and were tested on INSTRON 4206 tensile testing machine (ISO 6892:1998). Charpy impact tests were performed on standard CVN specimens (ISO 148:1983, size 10 × 10 × 55 mm, the notch of the specimen being perpendicular to the rolling-plane direction.) at room temperature using a JB-30A impact test machine. For both tensile and impact testing, three specimens were tested for each condition, and average values were reported. Vickers microhardness was measured using a Vickers hardness tester (HMV-2, SHIMADZU, Japan) using 9.8 N load. An average hardness of three indented fields for each sample was reported. The steel was polished and etched in a 2 pct natal solution, and the microstructure of the longitudinal transverse (L-T) plane was observed by optical microscope, SEM, and TEM (200CX and 2010F Hitachi, Tokyo).

3. Results

3.1 The Effect of Nb on the Dynamic Continuous Cooling Transformation of the F_{GBA}/B_G Steels

Figure 1 and 2 shows the dynamic CCT curves and the microstructure under different cooling rate of the experimental steels. It is found that F_{GBA}/B_G duplex microstructure can be obtained between 1 and 15 °C/s for No. 1 steel without Nb, between 0.4 and 10 °C/s for No. 2 steel with 0.06% Nb. The CCT curve shifts to lower position when 0.06% Nb was added. The ferrite and bainite transformation start temperature (Ar3 and Bs, respectively) of No. 2 steel are reduced to some degree compared to those of No. 1 steel without Nb addition. The volume fraction of ferrite decreases and the grain size is refined with 0.06% Nb addition. Such as under 1 °C/s, the volume fraction of ferrite is 73% for No. 1 steel, and 40% for No. 2 steel, respectively, and the grain size of ferrite is refined from 20 to 10 μm on average with 0.06 wt.% Nb addition, as shown in Fig. 2(a) and (b).

Table 2 shows Vicker hardness (HV) and corresponding thickness of water-quenched steel for different cooling rates. The relationship between cooling rate and thickness was obtained by finite element simulation. It is found that the Vicker hardness of No. 2 steel is higher than that of No. 1 steel at the same cooling rate. The difference on HV is more obvious when the cooling rates are higher.

3.2 The Effect of Nb on the Microstructure and Mechanical Properties of As-Rolled F_{GBA}/B_G Steels

Figure 3 shows the mechanical properties of No. 1 and No. 2 steels. It is found that with addition of 0.06 wt.% Nb, the tensile and yield strength increase by 21.4% (164 MPa) and 32.3% (181 MPa), respectively. The yield ratio increases a little and still is 0.8 for No. 2 steel. The impact energy increases by 62%, from 93 to 151 J.

Figure 4 shows the SEM and OM microstructure of as-rolled No. 1 and No. 2 steels, respectively. According to the nucleation position, the ferrite is classified to grain boundaries allotriomorphic ferrite (F_{GBA}) and intragranular idiomorphic ferrite (IF). Allotriomorphic ferrite usually formed on prior austenite grain boundaries during cooling below the Ar3 temperature. The ferrite nuclei have a Kurdjumov-Sachs (K-S) orientation relationship with one austenite grain and grow into the adjacent austenite grain with which they should normally have a random orientation relationship. At some lower temperature, ferrite may begin to nucleate on inclusions inside the austenite grains and this is termed intragranular IF. For No. 1 steel, the microstructure is composed of ferrite and

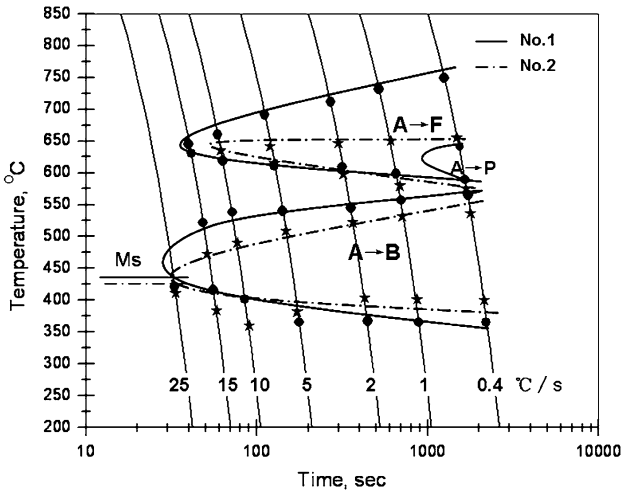

Fig. 1 Dynamic CCT curves of No. 1 and No. 2 F_{GBA}/G_B steels (F_{GBA}, grain boundary allotriomorphic ferrite; B_G, granular bainite; A, austenite; F, proeutectoid ferrite; B, bainite)

Table 1 The chemical compositions of the experimental steels

	C	Mn	Si	Nb	P	S	N	Fe
No. 1	0.06-0.08	2.0-3.0	0.6-0.9	···	0.0065	0.0052	0.0022	Bal
No. 2	0.06-0.08	2.0-3.0	0.6-0.9	0.06	0.0069	0.0081	0.0025	Bal

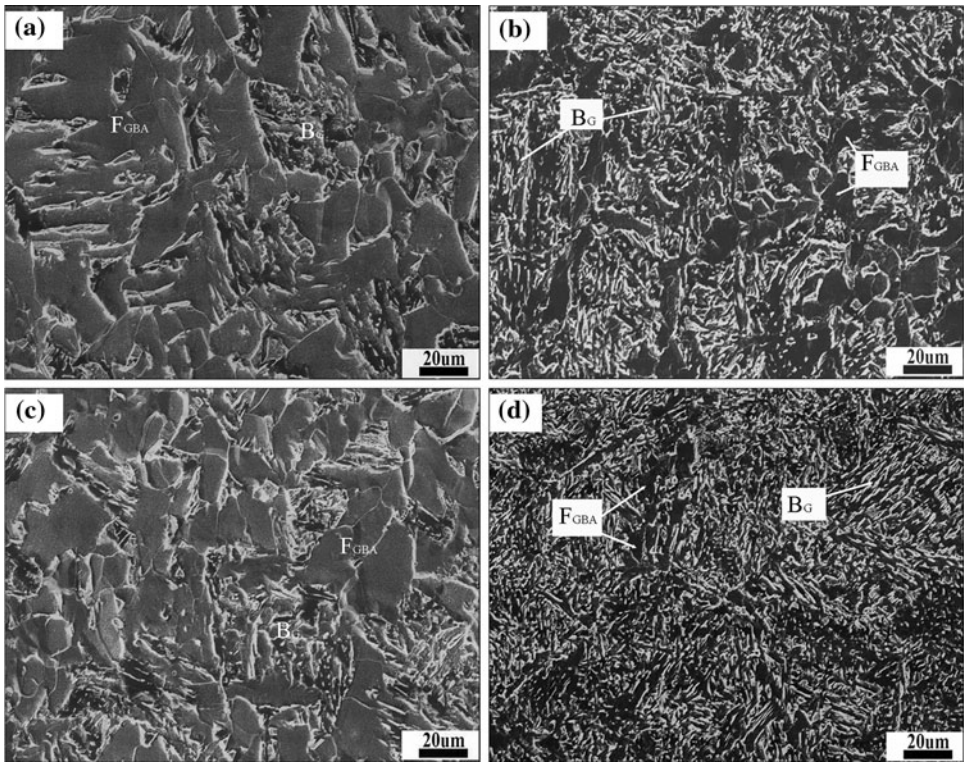

Fig. 2 Microstructure of F_{GBA}/B_G steels No. 1 (a, c) and No. 2 (b, d) for cooling rate of 1 °C/s (a, b), 10 °C/s (c, d)

Table 2 Vicker hardness (HV) and corresponding thickness of water quenched steel plate for different cooling rate

Cooling rate, °C/s	Corresponding thickness of steel plate, mm	Hardness (HV)		
		No. 1 steel	No. 2 steel	Difference
0.4	200	171 ± 2.3	195 ± 2.9	24 ± 3.7
1	120	184 ± 4.5	205 ± 2.1	21 ± 4.9
2	100	196 ± 2.1	219 ± 1.6	23 ± 2.6
5	60	204 ± 3.1	235 ± 1.2	31 ± 3.3
10	30	212 ± 1.2	250 ± 1.7	38 ± 2.1
15	25	234 ± 2.1	277 ± 1.7	43 ± 2.7
25	20	266 ± 1.7	311 ± 2.6	45 ± 3.1

B_G, and the ferrite including F_{GBA} and IF is predominantly polygonal or quasi-polygonal. The volume fraction of ferrite is about 30%, and the grain size is about 10 μm on average. On the other hand, for No. 2 steel, the microstructure is composed of ferrite, B_G, and martensite. The volume fraction of ferrite is below 9%, and the ferrite mainly has acicular structure which can divide the prior austenite grains. The grain size of F_{GBA} is about 5 μm in width, and that of IF is below 3 μm in width.

4. Discussions

The equilibrium solubility (wt.%) of Nb (C, N) in austenite can be calculated by the solid solubility equation (Ref 17)

$$\text{Log}\,[\text{Nb}] \cdot ([\text{C}] + 12[\text{N}]/14) = 2.06 - 6700/T$$

It is found that the 0.06 wt.% Nb in No. 2 steel is almost completely in solid solution. Figure 5 shows the TEM image and energy dispersive x-ray (EDX) spectroscopy analysis of

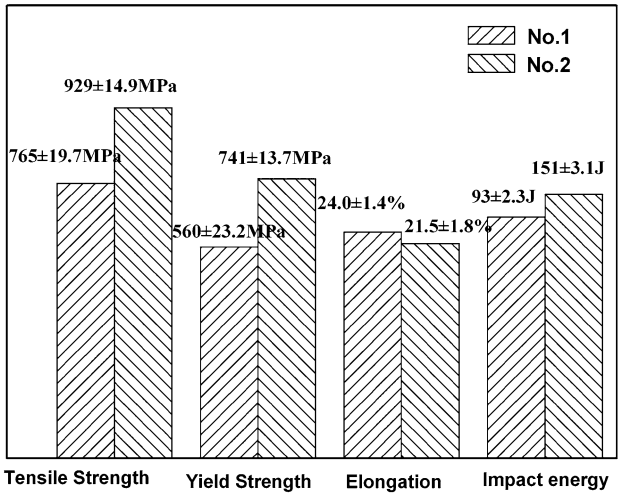

Fig. 3 Mechanical properties of No. 1 and No. 2 steels

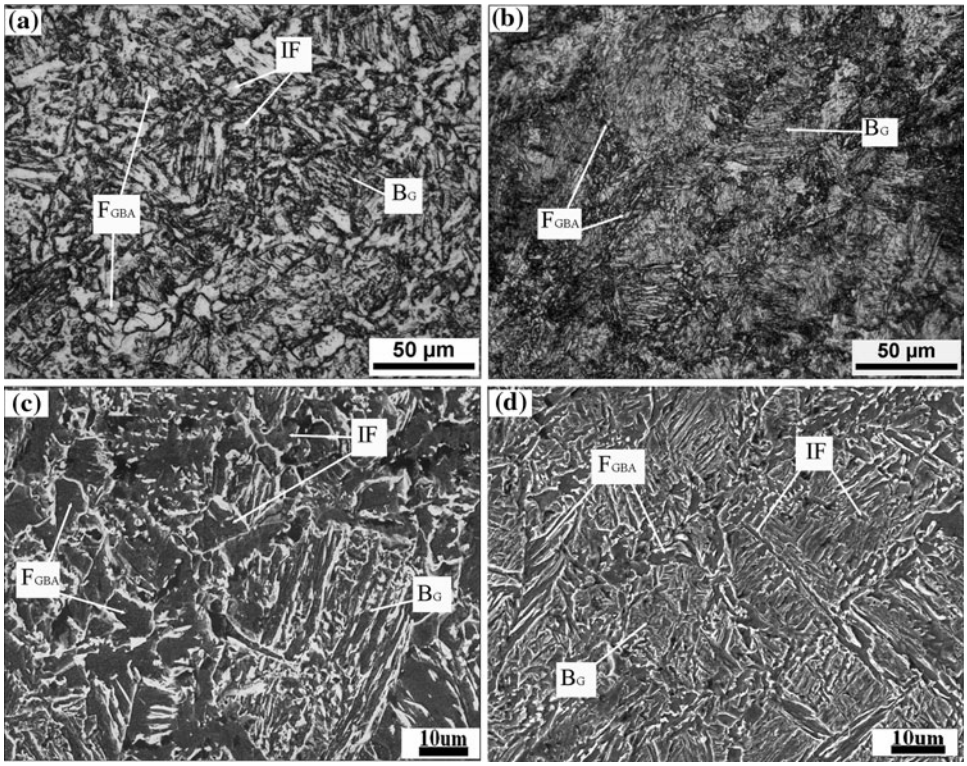

Fig. 4 OM (a, b) and SEM (c, d) images of F_{GBA}/B_G steel No. 1 (a, c) and No. 2 (b, d) after hot rolling and water quenching

carbon replica specimen of No. 2 steel. As shown in Fig. 5, only a few fine Nb(C, N) particles with size of about 20 nm are observed in as-rolled No. 2 steel. That is to say, the dissolution of Nb is sufficient and the precipitation of Nb(C, N) is rather scarce when 0.06 wt.% Nb was added.

4.1 The Effect of Nb on Ar3 of F_{GBA}/B_G Steel

The effect of Nb on the $\gamma \rightarrow \alpha$ transformation has been well established. Lee and Lee (Ref 18) suggested that solute Nb strongly segregates at the γ/α interphase boundary and reduces ferrite growth rate due to solute drag effect. On the other hand, Nb(C, N) precipitates in austenite accelerate the ferrite transformation because they could act as potential nucleation sites. In this study, the Ar3 of No. 2 with 0.06% Nb was lower than that of No. 1 with Nb-free, so it is concluded that solute Nb plays a leading role on Ar3. Killmore and co-workers (Ref 19) reported that Ar3 decreased by 10 °C per 0.01% dissolved Nb for the steels containing 0.031 and 0.04% Nb. Hong et al. (Ref 20) reported that Ar3 decreased by 7.4 °C per 0.01% dissolved Nb for 0.052% Nb. All the result of Ar3 mentioned above were determined under the same condition that the specimens with diameter of 10 mm were reheated at 1250 °C for 5 min and cooled at 2 °C/s without deformation. Wang and co-workers (Ref 21) reported that Ar3 started to increase when the Nb content is higher than 0.023%, and the Ar3 decreased by about 6 °C per 0.01% Nb for steels containing 0.04% Nb after with a true strain of 0.693 (50% reduction) at 900 °C. According to Fig. 2, it is found that Ar3 of No. 2 with 0.06% Nb at a rate of 2 °C/s is lowered by 64 °C after 30% deformation at 850 °C. The effect of Nb on Ar3 in this present work is more obvious than that in former works, which is due to the effect of Mn on increasing the solubility of Nb(C, N)

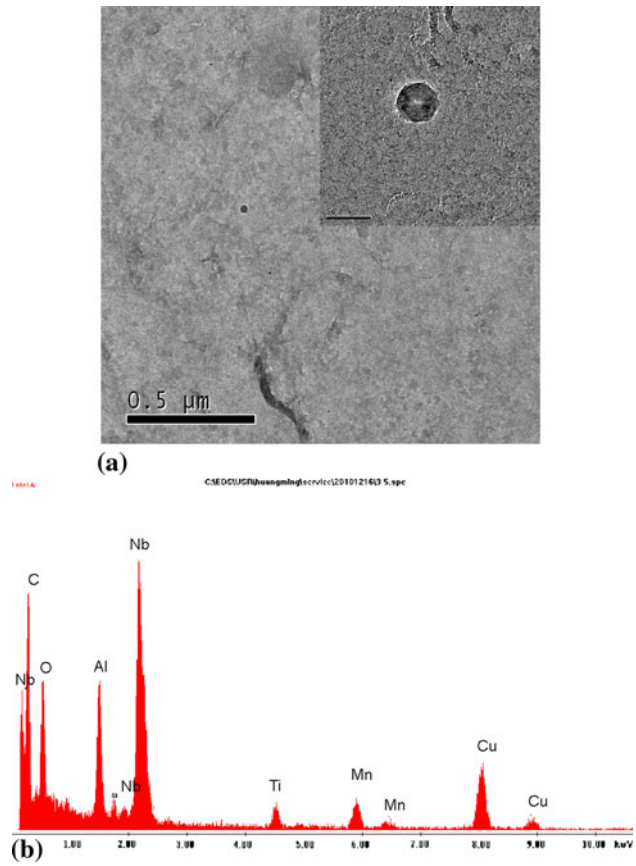

Fig. 5 Nb(C, N) particles distribution in No. 2 steel with 0.06 wt.% Nb, (a) the distribution and magnification of Nb(C, N) particles, (b) EDX spectra of the Nb(C, N) particle

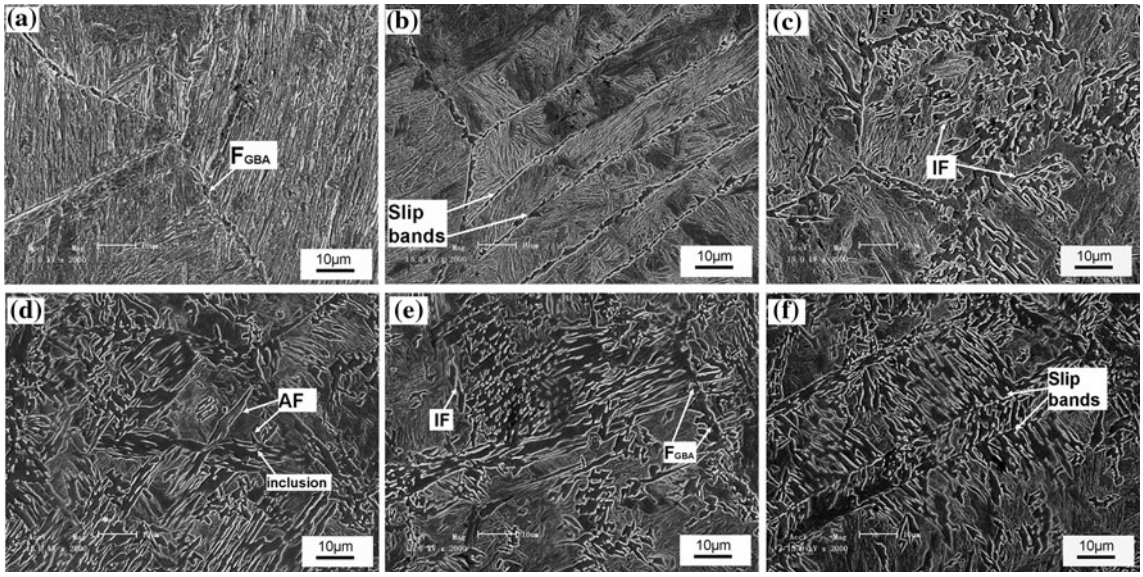

Fig. 6 The formation process of ferrite and bainite in No. 2 steel, (a) grain boundary allotriomorphic ferrite (F_{GBA}), (b) ferrite nucleating at slip bands, (c) intragranular ferrite (IF), (d) acicular ferrite, (e) bainite growing from F_{GBA}, and (f) bainite growing form slip bands

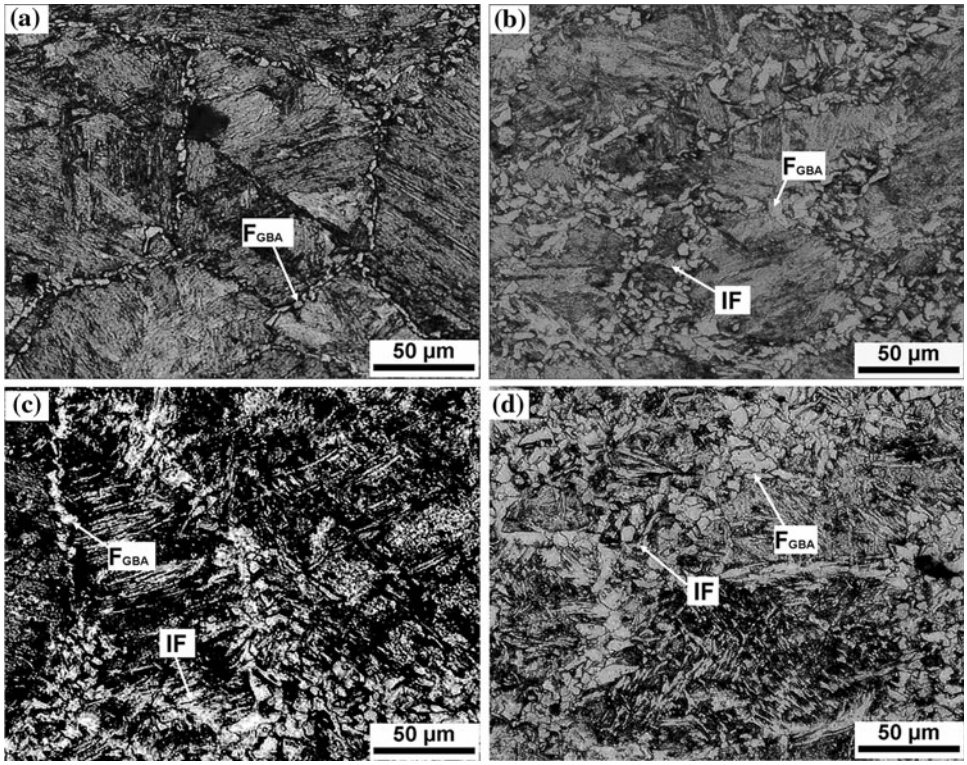

Fig. 7 The formation process of ferrite in No. 1 steel, water quenching from (a) 700, (b) 670, (c) 650, and (d) 600 °C (the grain boundary allotriomorphic ferrite (F_{GBA}) dominates during the transformation process)

particles in austenite and delaying the precipitation of Nb(C, N) particles (Ref 22).

4.2 The Effect of Nb on Microstructure Evolution of F_{GBA}/B_G Steel

In order to investigate the effect of Nb on microstructure evolution of F_{GBA}/B_G steel, microstructure observations were performed on samples water quenched from the different temperature. The samples were cooled at the cooling rate of 10 °C/s after the deformation at 850 °C, and water quenched from 700, 670, 650, 600, 550, and 500 °C. For No. 2 steel, the ferrite starts to nucleate on the prior austenite grain boundaries at 670 °C, as shown in Fig. 6(a). At later stage of transformation at 650 °C, the ferrite nucleates on the deformation bands which divide the prior austenite grain into some parts (Fig. 6b).

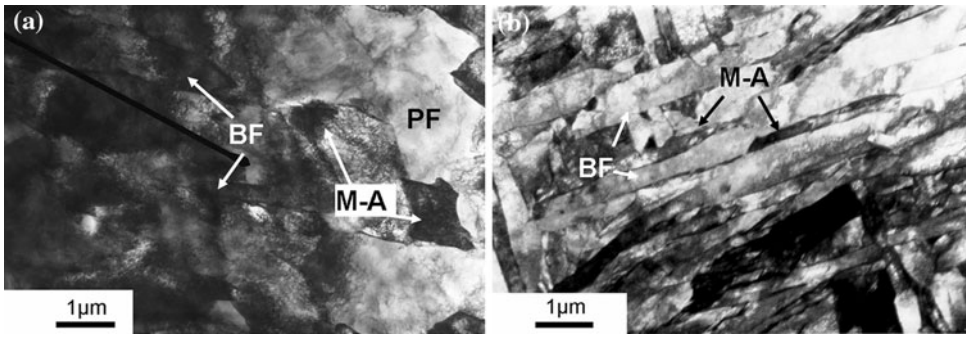

Fig. 8 TEM image of F_{GBA}/B_G steel after hot rolling and water quenching (a) No. 1 steel with Nb-free and (b) No. 2 steel with 0.06 wt.% Nb

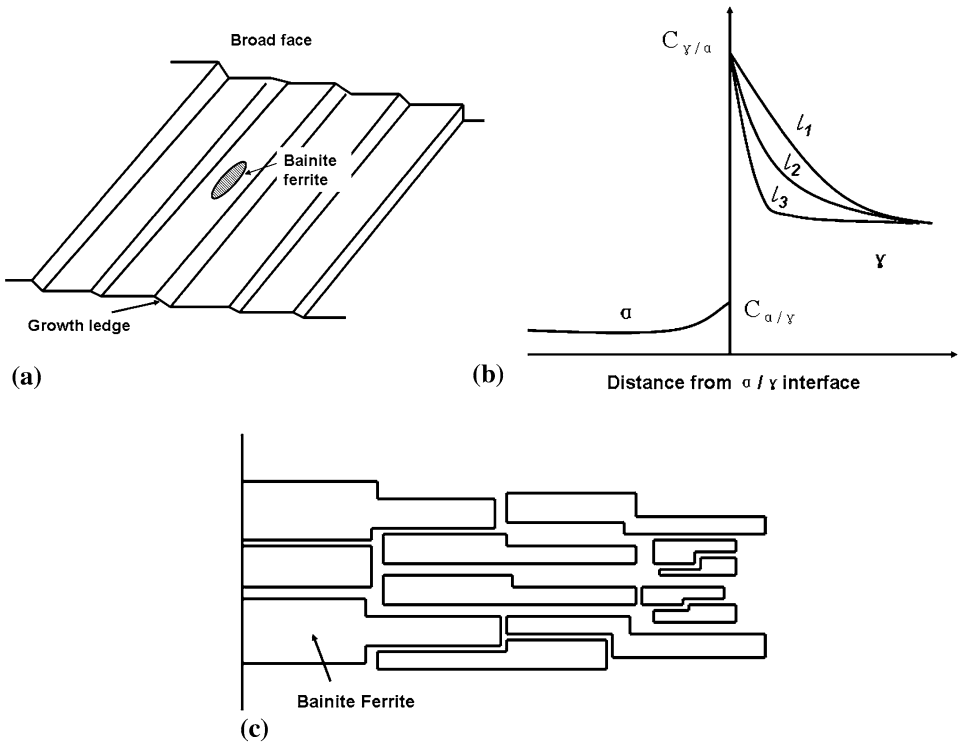

Fig. 9 Schematics of sympathetic nucleation-ledgewise growth model (a) nucleation on the broad face of growth ledge, (b) concentration profile of α/γ interface area, and (c) model of bainite ferrite structural units

The formation of intragranular ferrite is observed at 600 °C (Fig. 6c), and the ferrite nucleating on prior austenite grain boundaries grows into austenite grain with acicular structure (Fig. 6c). The acicular ferrite is observed at 500 °C (Fig. 6d) in the bainite transformation temperature range. At the same time, at stage of transformation at 500 °C, the bainite ferrite grows from prior austenite grain boundaries and deformation bands, as can be seen in Fig. 6(e) and (f), but the growth terminates when bainite ferrite meets with the intragranular ferrite (Fig. 6e). On the other hand, in case of No. 1 steel, the volume fractions of ferrite nucleating on slip bands and intragranular ferrite are obvious less than those for No. 2 steel, as shown in Fig. 7, which is water quenched from 700 (Fig. 7a), 670 (Fig. 7b), 650 (Fig. 7c), and 600 °C (Fig. 7d). OM images with low magnification are employed due to the coarser-grain size in No. 1 steel.

It is well known that Nb can promote the formation of deformation bands and dislocation structures with hot deformation. It is because that the small Nb(C, N) can pin down dislocation and Nb in solid solution atomic state segregating at dislocation can form "Cottrell air mass" to reduce the climbing velocity of edge dislocation (Ref 23). The deformation bands and dislocation structures inside the deformed austenite grains favor the nucleation of intragranular ferrite. The formation of intragranular ferrite can divide the prior austenite grain and contribute to the refinement.

4.3 The Effect of Nb on Microstructure Refinement of F_{GBA}/B_G Steel

Figure 8(a) shows TEM image of No. 1 steel as rolled. The polygonal ferrite with dark chunky-shaped M/A constituents is observed. The size of M/A constituents is about 1 μm. Figure 8(a) shows bainite ferrite has higher dislocation density than polygonal ferrite. The size of the bainite ferrite laths is about 1 μm in width. A change in microstructure is observed with 0.06 wt.% Nb addition, as shown in Fig. 8(b). The chunky-shaped M/A constituents dispersing among polygonal ferrite are suppressed, substituted by club-shaped M/A constituents distributing in parallel direction between the bainite ferrite laths. The width of M/A constituents varies from 50 to 300 nm, and the length varies from 0.5 to 3 μm. The size of the bainite ferrite laths is about 0.5 μm in width.

It is suggested that structure refinement induced by 0.06 wt.% Nb addition could be explained by sympathetic nucleation and ledgewise growth mechanism (Ref 24). Sympathetic nucleation is defined as "the nucleation of a precipitate crystal at an interphase boundary of a crystal of the same phase when these crystals differ in composition from their matrix phase throughout the transformation process." The migrating interface is showed in Fig. 9(a). In the course of thickening of a plate, the carbon concentration of ferrite and austenite in the vicinity of the interface around a growth ledge are under para-equilibrium condition and represented by $C\alpha/\gamma$ and $C\gamma/\alpha$, respectively (Fig. 9b). The growth of α is completely controlled by volume diffusion of carbon in γ. A large amount of carbon will be excluded into the matrix at the front of the migrating ledge and thus the carbon concentration profile will change from l_1 to l_2, and then to l_3, i.e., the carbon gradient in γ decreases and then the lateral migration rate of ledge decreases. Thus, the embryo on the broad face of ferrite will not be overrun by growth ledge and survive. Sympathetic nucleation associated with ledgewise growth mechanism is considered to be responsible for the various arrangements of fine structural units within a bainite plate or lath. It is known that the activity of carbon is reduced due to the strong interaction between carbon and niobium, the diffusion rate of carbon in γ decreases and then the lateral migration rate of ledge decreases. Furthermore, solute Nb is heavily segregated at γ/α phase boundaries and reduces the ferrite growth rate. When the lateral migration of ledge stopped, sympathetic nucleation would occur, and the fine structure units were obtained. The shorter the time for ledge migration was, the finer the structure units were obtained (Fig. 9c).

In summary, the increase in strength and impact energy with 0.06 wt.% addition is relate to the refinement of the structure, including F_{GBA}, B_G clusters, bainite ferrite laths, and M/A constituents. Some studies showed, for F_{GBA}/B_G duplex phase, the tensile strength depends on the volume fraction and morphology of M/A constituents, and yield strength depends on strength of ferrite, respectively (Ref 25). The increase in strengthening phases, such as M/A constituents and martensite phase, reinforces tensile strength of F_{GBA}/B_G steel with 0.06 wt.% Nb. The refinement of F_{GBA}, IF, and bainite ferrite is the dominating reason for the improvement of yield strength.

5. Conclusions

(1) The addition of 0.06 wt.% Nb increased the hardenability of the F_{GBA}/B_G steel, suppressed the transformation of $\gamma \rightarrow \alpha$, refined the size of F_{GBA}, promoted the granular bainitic transformation, reduced the bainitic transformation start temperature, and refined the granular bainite including its bainitic ferrite and M/A constituents.

(2) With the addition of 0.06 wt.% Nb, the yield strength increases from 560 to 765 MPa, and the impact energy increases from 93 to 151 J, respectively, after deformed by 21% at 800 °C, water quenched to 450 °C, and then air cooling to room temperature.

(3) It is suggested that the increase in strength and impact energy with 0.06 wt.% addition can be attributed to the refinement of the structure, including F_{GBA}, B_G clusters, bainite ferrite laths, and M/A constituents.

References

1. K. Hulka, F. Hesterkamp, and L. Nachtel, Ed., *Processing, Microstructure and Properties of HSLA Steels*, TMS, Warrendale, PA, 1988, p 153
2. S.W. Thompson, D.J. Colvin, and G. Krauss, Continuous Cooling Transformation and Microstructure in a Low Carbon, High Strength Low Alloy Plate Steel, *Metall. Trans. A Phys. Metall. Mater. Sci.*, 1990, **21A**, p 1493–1507
3. S.W. Thompson, D.J. Colvin, and G. Krauss, Austenite Decomposition During Continuous Cooling of a HSLA 80 Plate Steel, *Metall. Mater. Trans. A Phys. Metall. Mater. Sci.*, 1996, **27A**, p 1561–1571
4. D.P. Dunne, S.S. Ghasemi, D. Banadkouki, and D. Yu, Isothermal Transformation Products in a Cu-Bearing High Strength Low Alloy Steel, *ISIJ Int.*, 1996, **36**, p 324–333
5. P.C.M. Rodrigues, E.V. Pereloma, and D.B. Santos, Mechanical Properties of an HSLA Bainitic Steel Subjected to Controlled Rolling With Accelerated Cooling, *Mater. Sci. Eng. A*, 2000, **283**, p 136–143
6. P.K. Ray, R.I. Ganguly, and A.K. Panda, Optimization of Mechanical Properties of an HSLA-100 Steel Through Control of Heat Treatment Variables, *Mater. Sci. Eng. A*, 2003, **346**, p 122–131
7. A. Ghosh, S. Das, S. Chatterjee, and P. Ramachandra Rao, Effect of Cooling Rate on Structure and Properties of an Ultra-Low Carbon HSLA-100 Grade Steel, *Mater. Charact.*, 2006, **56**, p 59–65
8. H.-S. Fang, Y.-K. Zheng, X.-Y. Chen, R.-F. Zhao, and X. Zhou, Novel Air-Cooled Bainitic Steels, *J. Met.*, 1998, **40**(3), p 51 (in Chinese)
9. P.-G. Xu, H.-S. Fang, and B.-Z. Bai, New Duplex Microstructure of Grain Boundary Allotriomorphic Ferrite/Granular Bainite, *Iron Steel Res. Int.*, 2002, **9**(2), p 33
10. P.G. Xu, B.Z. Bai, F.X. Yin, H.S. Fang, and K. Nagai, Microstructure Control and Wear Resistance of Grain Boundary Allotriomorphic Ferrite/Granular Bainite Duplex Steel, *Mater. Sci. Eng. A*, 2004, **385**, p 65–73
11. J.-P. Wang, Z.-G. Yang, B.-Z. Bai, and H.-S. Fang, Grain Refinement and Microstructural Evolution of Grain Boundary Allotriomorphic Ferrite-Granular Bainite Steel After Prior Austenite Deformation, *Mater. Sci. Eng. A*, 2004, **369**, p 112–118
12. H.S. Fang, C. Feng, B.Z. Bai et al., Creation of Air-Cooled Mn Series Bainitic Steels, *J. Iron Steel Res. Int.*, 2008, **15**(6), p 1–9
13. S. Shanmugam, N.K. Ramisetti, R.D.K. Misra, T. Mannering, D. Panda, and S. Jansto, Effect of Cooling Rate on the Microstructure and Mechanical Properties of Nb-Microalloyed Steels, *Mater. Sci. Eng. A*, 2007, **460**, p 335–343
14. K.L. Lee, J.K. Lee, K.B. Kang, and O. Kwon, Mathematical Modelling of Transformation in Nb Microalloyed Steels, *ISIJ Int.*, 1992, **32**(3), p 326–334
15. C. Fossaert, C. Rees, T. Maurickx, and H.K.D.H. Bhadeshia, The Effect of Niobium on the Hardenability of Microalloyed Austenite, *Metall. Trans. A Phys. Metall. Mater. Sci.*, 1995, **26A**, p 21–30
16. N. Shams, The Effect of Niobium on the γ/α Transformation in Low Carbon Manganese Steels, *Trans. ISS, I & SM*, 1990, **9**, p 51
17. K.J. Irvine, F.B. Pickerin, and T. Gladman, Grain-Refined C-Mn Steels, *J. Iron Steel Int.*, 1967, **205**(2), p 161

18. K.J. Lee and J.K. Lee, Modelling of γ/α Transformation in Niobium-Containing Microalloyed Steels, *Scr. Mater.*, 1999, **40**(7), p 831–836
19. P.A. Manohar, T. Chandra, and C.R. Killmore, Continuous Cooling Transformation Behaviour of Microalloy Steels Containing Ti, Nb, Mn and Mo, *ISIJ Int.*, 1996, **36**(12), p 1486–1491
20. S.C. Hong, S.H. Lim, H.S. Hong, K.J. Lee, D.H. Shin, and K.S. Lee, Effects of Nb on Strain Induced Ferrite Transformation in C-Mn Steel, *Mater. Sci. Eng. A*, 2003, **355**(1–2), p 241–248
21. X.Q. Yuan, Z.Y. Liu, S.H. Jiao, L.Q. Ma, and G.D. Wang, The Onset Temperatures of Gamma to Alpha-Phase Transformation in Hot Deformed and Non-Deformed Nb Micro-Alloyed Steels, *ISIJ Int.*, 2006, **46**(4), p 579–585
22. M.G. Akben, I. Weiss, and J.J. Jonas, Dynamic Precipitation and Solute Hardening in A V Microalloyed Steel and Two Nb Steels Containing High Levels of Mn, *Acta Metall.*, 1981, **29**(1), p 111–121
23. Q.B. Yu, Z.D. Wang, X.H. Liu, and G.D. Wang, Effect of Micro Content Nb in Solution on the Strength of Low Carbon Steels, *Mater. Sci. Eng. A*, 2004, **379**, p 384–390
24. H.S. Fang, J.B. Yang, Z.G. Yang, and B.Z. Bai, The Mechanism of Bainite Transformation in Steels, *Scr. Mater.*, 2002, **47**, p 157–162
25. F.Y. Xu, ''Study on the Formation, Strength and Toughness of Duplex Phase Structure Consist of Ferrite and Island,'' PhD Thesis, Tsinghua University, Beijing, China, 2009 (in Chinese)